TECHNICKÁ UNIVERZITA V LIBERCI
Fakulta mechatroniky, informatiky
a mezioborových studií

PETR HOŠEK

AUTOMATION OF MEASUREMENT OF DYNAMIC RESPONSE OF VALVETRAINS

Report of the Phd Thesis

Technical university of Liberec, 2011

Phd Thesis

Automation of measurement of dynamic response of valvetrains

Automatizace měření dynamické odezvy ventilových rozvodů

Author: Petr Hošek
(petr.hosek@tul.cz)
Supervisor: Doc. Ing. Antoním Potěšil, CSc.
Study programme: P2612 Electrotechnics and informatics
Field of study: 2612V045 Technical Cybernetics
Department: Faculty of Mechatronics, Informatics and Interdisciplinary studies,
Institute of New Technologies and Applied Informatics,
Technical University of Liberec,
Studentská 2, 461 17 Liberec 1, Czech Republic

Abstract

This thesis describes the development of a new generation of an apparatus for automated measurement of the dynamic response of valvetrains and presents analyses of the measured data. It focuses on, as a key component, the development of the measurement software and the algorithm for signal drop-out recognition that made this fully automated measurement possible. As a result the time of the measurement was drastically reduced thus increasing the throughput and improving the repeatability. The construction of the device and the software are versatile and applicable in several other measurement setups.

An implementation of Siemens USS protocol into LabVIEW is presented, as there was a permanent demand from the community of users to have the native LabVIEW implementation. The protocol is used as a communication interface to drive Siemens frequency inverter. By using the connected electromotor, the frequency inverter drives the crankshaft of the combustion engine. The encountered problems and their solutions are mentioned.

The next study introduces an algorithm for the recognition of signal drop-outs developed particularly for measurements of valvetrain kinematics performed by laser Doppler vibrometer. Signal drop-outs are the result of low amplitude levels of the Doppler signal due to changes in the speckle noise during tilt and rotation of valve. The recognition algorithm is needed in order to save data that are not affected by this phenomenon. Such an algorithm increases the throughput of the engine test stand and decreases the time needed for the following evaluation of the valvetrains of combustion engines. The work shows the most common encountered drop-outs and their characteristics and locations. It presents an automatic separation algorithm for the measured signal so that the drop-out recognition tests can be aimed at specific data intervals (valve opening, valve closing, etc.) with specifically set parameters of the algorithm.

Advanced techniques for real-time parallel measurement, software controlling, data acquisition, multi-instrument communication and post-processing were combined and are described. They assure the automation and certain level of intelligence and safety of the developed system.

To evaluate the developed system and to show its overall capabilities, first the standard ŠKODA 1.2 HTP engine with OHC valvetrain was measured. Second the low-friction valvetrain for the same engine was examined and compared. A direct comparison of valve acceleration calculated while presuming constant camshaft speed and the approach that benefits from the measured speed fluctuations was carried out. It was expected that by using the speed fluctuations for the velocity as well as acceleration normalization and valve acceleration computation, the results would be more precise.

Finally, we carried out a comparison of the measured data of the half-engine setup and the partial-engine setup. The half-engine setup utilizes nearly a full-engine assembly. The partial-engine setup, on the other hand, utilizes only the head and the head cover and the related valvetrain components. This setup is commonly used in the automotive industry to simplify valvetrain tests. It was expected to deliver values close to the half-engine setup, although no direct comparison has been published. The results show a wide variety of different analyses that can be performed from a single measurement.

Keywords: valvetrain, speckle noise, signal drop-out, laser Doppler vibrometry, USS protocol, data acquisition, automation

Abstrakt

Tato práce popisuje návrh a vývoj nové generace testovacího zařízení pro automatizované měření dynamické odezvy ventilových rozvodů a předkládá analýzy naměřených dat. Zaměřuje se na vývoj měřícího softwaru a algoritmů pro detekci výpadků dopplerovského signálu jakožto klíčových částí měřícího řetězce, které umožnily toto měření plně automatizovat. V konečném důsledku byl čas měření významně zkrácen, a tudíž byla zvýšena efektivita testovacího zařízení a opakovatelnost měření. Zařízení je koncipováno jako mnohoúčelové a použitelné i v jiných odvětvích měření spalovacích motorů.

V textu práce je popsána naše implementace USS protokolu do LabVIEW, jež byla dlouhodobě nevyřešena a zároveň velmi žádána. Protokol je použit jako rozhraní ke komunikaci s frekvenčním měničem Siemens. Frekvenční měnič pak řídí elektromotor, který pohání spalovací motor při měřeních. V práci jsou rovněž zmíněny problémy, které se při implementaci protokolu objevily a jejich řešení.

Podstatná část práce popisuje algoritmus pro identifikaci výpadků signálu, který byl vyvinut pro měření kinematiky ventilů pomocí laserového dopplerovského vibrometru. Tyto výpadky signálu se objevují při nízké amplitudě dopplerovského signálu jakožto důsledek dynamických změn speckle šumu během rotace a náklonu ventilu. Detekční algoritmus ukládá pouze data nepostihnutá tímto jevem, což výrazně snižuje čas nutný k následné analýze naměřených dat. V práci jsou uvedeny nejčastější typy výpadků, jejich vlastnosti a umístění. Jsou popsány vytvořené algoritmy sloužící k automatické separaci měřeného signálu. Toto umožňuje přesnější zacílení parametrů testů rozpoznávajících výpadky v daném intervalu (otevírání ventilu, zavírání ventilu atd.).

K zajištění automatizace, bezpečnosti a jisté inteligence vytvořeného systému bylo nutné kombinovat pokročilé techniky pro paralelní sběr dat, komunikaci s vícero přístroji a zpracování dat.

K ověření schopností systému byly proměřeny dva OHC ventilové rozvody – nejprve standardní sériový ŠKODA 1.2 HTP a následně lehkoběžná verze tohoto rozvodu. Výsledky obou rozvodů byly porovnány v několika detailních analýzách. Bylo rovněž provedeno porovnání dvou přístupů k výpočtu zrychlení ventilu z naměřených dat rychlosti. Běžně je pro tyto účely zanedbávána nerovnoměrnost otáčení vačkového hřídele. Jelikož náš systém je schopen měřit průběh rychlosti otáčení hřídele, bylo toto do výpočtu zahrnuto. Předpokládalo se, že tato informace zpřesní výsledek výpočtu.

Na závěr bylo provedeno měření tzv. částečného uspořádání motoru (partial-engine setup). Naměřené kinematické veličiny ventilů byly porovnány vůči hodnotám z předchozího měření na maketě motoru (half-engine setup), která se skládá z téměř úplného motoru. Naproti tomu částečné uspořádání využívá pouze hlavu válců, víko a nezbytně související části rozvodu. Toto uspořádání je běžně používáno v automobilovém průmyslu k zjednodušení měření rozvodů. Ačkoli se předpokládá, že poskytuje měřené hodnoty blízké hodnotám z měření na maketě, nebylo přímé porovnání nikdy publikováno (s ohledem na znalosti autora). Výsledky ukazují širokou škálu analýz, jež mohou být provedeny z jednoho měření.

Klíčová slova: ventilový rozvod, speckle, výpadky signálu, laserová dopplerovská vibrometrie, USS protokol, sběr dat, automatizace

Contents

1 Introduction

1.1 Background and motivation of the work

The internal combustion (IC) engine has been evolving for almost one and half centuries (1866, Daimler, Benz, first car with combustion engine). Nevertheless, the keystones still remain the same. We still use cams and valves while the research focused on replacing those parts with electromagnetic elements is in progress.

In the electromagnetic actuation concept, the opening and closing of the valve is obtained by alternatively energizing upper and lower magnets with an armature connected to the valve. This actuating principle offers maximum flexibility and dynamic response in valve control, but despite a decade of significant development efforts, the main drawbacks of the concept (it being not fail-safe and its high energy absorption) have not been fully overcome [1]. Thus those elements remain electromechanical [2] or hydraulically-actuated [3] as in case of the MultiAir Technology from Fiat [4].

Testing is an important part of the design process of each individual component. First, it enables checking of the correct functionality while at the same time monitoring the critical values that might negatively influence the lifetime of the final product. The measurement of the valve displacement and velocity is a fundamental part of the validation of the valvetrain design. With high speeds the eigenfrequency and stiffness of each part, the mass distribution, resonance or friction begin to play an important role that may lead to changed cylinder fluid dynamics. Phenomena like valve float and valve bounce may appear. Valve float can be observed when the inertial force of the valvetrain components exceeds the spring force of the valve springs, thus allowing components to separate. In addition, valve float causes the valve to exceed the maximum lift of the kinematic motion and close with an abnormally high velocity [5]. Valve bounce occurs when the valve closes against the seat with such a high velocity that it physically bounces off the seat and remains open as the piston begins the compression cycle [5], [6]. If the valve is repeatedly seated with too high velocity (so called impact velocity [7]) the seat can be worn off. Contact fatigue or other damage may appear. Due to resulting leakage, valve heat dissipation is not ensured and local heat load increases. The valve can even melt. To prevent or minimize those effects we have to have an apparatus to discover the conditions of their occurrence.

High speed Laser Doppler Vibrometry (LDV) has become a standard measurement technique for obtaining the kinematics of the valves [6], [8]. The main reason is that the technique is non-contact and offers information about both the valve displacement (using the fringe counting technique [9], [10]) and the valve velocity (based on the Doppler effect) up to high engine speeds. The LDV technique also has its drawbacks. It is sensitive to dust and oil droplets that might appear during the measurement and demands precise focusing of the lenses. However, the main problems arising during the automation of the measurement are *speckle noise* and *signal drop-outs* [11], [12], [13].

The current measurement procedure of the valve kinematics is time consuming. The measurement has to be carried out over the given (operational) spectrum of the engine rpm. The higher frequencies tend to be more interesting for further processing so they are measured in detail with smaller rpm increment. Ideally all the valves (all cylinders, exhaust and intake valves) are examined. It might take a day to measure the response of a valvetrain with newly designed curvature of a cam or when new valve springs are used. To save time, usually only the valves closest and endmost to the camshaft drive are examined.

In industry it is necessary to have high throughput of the testbed, which results in inability to check the occurrence of the drop-out phenomenon in detail. This is partly because of the amount of the measured data and partly because some problematic parts can be discovered only after a very detail processing.

A fully-automated system which would significantly reduce the time needed for the complete analysis of the valvetrain components would be a great tool. Such a system has to offer prompt feedback for the design engineers, repeat measurement in case of recognition of signal drop-out and deliver as much information as possible from a single measurement.

1.2 Contribution of the thesis

To test and analyze the dynamics of the valvetrain is essential since it presents the part of the engine where even slight changes directly influence the engine setting, lifetime and fuel consumption [14].

The measurement system we designed and constructed can be called a new generation of the apparatus commonly used for the valve kinematics measurements [6], [8]. The systems described in the referenced papers are rather experimental and have their limitations. On the other hand, our apparatus is aimed at industry. It spans all of the engine's operational speeds and can operate with a half-engine or a partial-engine setup (partial-engine setup utilizes only the head and the head cover and the related valvetrain components). As described later, it also automatically compensates for slippage of the ribbed belt that is used to transfer the torque between the shaft of the electromotor and the combustion engine. Moreover, it is capable of a truly parallel measurement of the camshaft speed fluctuations, which can help to discover a faulty valvetrain component or to improve the precision of calculations that presume the speed of the shaft to be constant. Most of all, with the algorithm for LDV drop-out noise detection, the system is fully automated. It runs the measurement across predefined engine speeds, repeating if drop-out noise is detected and saving only the representative data for further processing.

With the constructed system, we carried out a measurement of the valvetrain kinematics and the camshaft speed fluctuations of engine in half setup and partial setup. The partial-engine setup is commonly used to make the measurement faster and cheaper, although no direct comparison of the measurement results has been presented before.

2 Design of the measurement apparatus

The apparatus for valvetrain testing is a very complex system spanning many different technical fields. It is designed to reproduce the functional conditions in cars.

At the beginning we have a combustion engine with a set up valvetrain and all the accessories so the dynamics of the valvetrain is preserved. When the measurement is finished we should have the desired characteristics (displacement and velocity of the valve) of the valvetrain under examination and shaft speed fluctuation curve.

2.1 Developed measurement system

The measurement system (Fig. 2.1) utilizes electromotor and frequency inverter with communication unit to drive it. The electromotor is used to drive the crankshaft of the combustion engine. Between the electromotor and the crankshaft the step-up gear is installed to allow the full range of measurement rpm, typically $rpm_{crank} = 0 – 6000$ rpm. The camshafts (DOHC) in the most common setup are connected to the crankshaft via a timing chain. The incremental encoder (IRC) is placed either at the end of the intake valve camshaft or the exhaust valve camshaft offering the information about the camshaft displacement and subsequently about the camshaft speed fluctuations and the actual speed of rotation. The cylinder head cover had to be modified to allow that. If needed, the IRC can also be mounted at the end of the crankshaft. The camshafts of the test engine were driven by the crankshaft using a timing chain with a reduction ratio of 1:2.

Apertures were milled into the place where pistons normally belong. The pistons were removed and in the created space the laser Doppler probes were installed. The original crankshaft was replaced with a modified straight ‘dummy’ shaft, only to drive the connected valvetrain and the oil pump. No gas forces or combustion forces occur in the measurement system. Excluding those forces, however, does not compromise the validity of the experimental data [15], [8]. In this thesis, we will refer to the assembly as a *half-engine setup*.

The measured valve is always equipped with retro-reflective tape which is placed at the center of the bottom side of the plate. One fiber optics laser probe is aimed at the tape and monitors the motion of the valve (measurement arm). It works as a transmitter and receiver at the same time. The second probe is aimed at the cylinder head (reference arm) itself which is also rigged with the tape. The probes are connected to a differential laser Doppler system which uses Mach-Zehnder interferometer design. The vibrations of the cylinder head arising during the measurement are subtracted from the motion of the valve. The measurement is thus more accurate. The connected laser vibrometer controller handles the evaluation of the incoming signals and outputs analog signals representing the displacement and velocity of the monitored valve. Those signals are connected to two channels of the data acquisition (DAQ) card. Only the component of motion along the optical axis of the instrument can be determined, so the two beams must be aligned parallel to the valve stem to have a correct measure [8].

The pulse signal from the IRC encoder is used as an external sampling source so the data are sampled depending on the actual cam displacement. The standard for this type of measurement is 720 pulses per revolution (ppr). This offers resolution 0.5° of the camshaft which is fine enough, preserves good readability, shows step changes in acceleration that can discover problematic parts and doesn’t pose a problem of handling huge amount of data. We also use higher resolutions (i.e. 1800 and 3600 ppr). Moreover, the IRC signal is used by the created controlling software to compensate slippage of the ribbed belt which is used to

transfer the torque between the shaft of the electromotor and the combustion engine. In addition, the IRC enables monitoring shaft speed fluctuations during one revolution of the camshaft. The reference signal (one impulse per rotation) serves as a trigger signal to start the data acquisition and reset the interferometer.

The main parts of the apparatus are embedded into a frame that was specially built for our purposes offering stability, rigidity, and minimizing the vibrations and the impact on the surrounding environment. It can hold common three cylinder and also four cylinder engines.

We also installed a system for oil heating and cooling which allows setting and monitoring of desired operating temperature as well as pressure sensing. The whole measurement is operated by developed software.

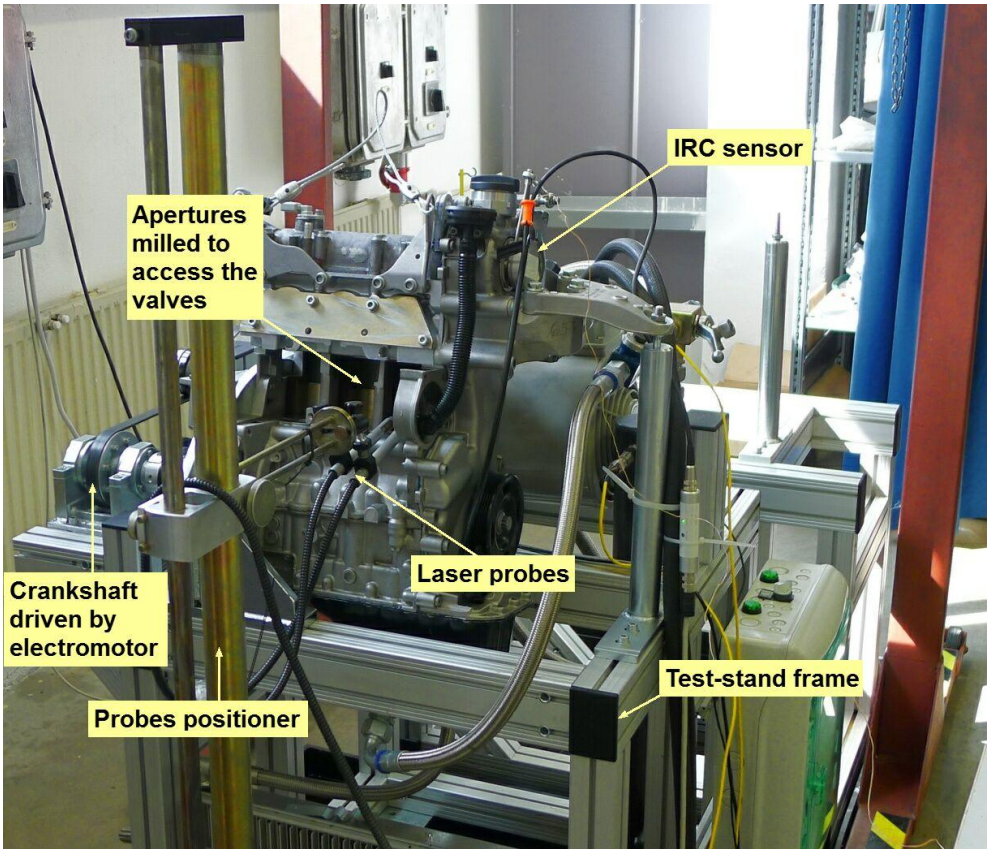

Figure 2.1 – Photo of the apparatus in half-engine setup

3 Algorithm for signal drop-out recognition in IC engine valve kinematics signal measured by laser Doppler vibrometer

We present an algorithm for the recognition of signal drop-out developed particularly for measurements of valvetrain kinematics. This algorithm is needed in order to save data that are not affected by a drop-out phenomenon and thus allow full automation of the measurement. Such an algorithm will increase the throughput of the engine test stand and decrease the time needed for the evaluation of the valvetrains of combustion engines. The work shows the most commonly encountered drop-outs and their characteristics and locations. It presents an automatic separation algorithm for the measured signal so that the drop-out recognition tests can be aimed at specific data intervals (valve opening, valve closing, etc.) with specifically set parameters of the algorithm.

3.1 Motivation for the drop-out recognition and phenomena affecting the valve kinematics signal

High speed Laser Doppler Vibrometry (LDV) has become a standard measurement technique for obtaining the kinematics of the valves [6], [8]. The main reason is that the technique is non-contact and offers information about both the valve displacement (using the fringe counting technique [9], [10]) and the valve velocity (based on the Doppler effect) up to high engine speeds. The LDV technique also has its drawbacks. It is sensitive to dust and oil droplets that might appear during the measurement and demands precise focusing of the lenses. However, the main problems arising during the automation of the measurement are *speckle noise* and *signal drop-outs.*

A speckle pattern is produced when the coherent waves of the incident laser beam are dephased during backscatter from a surface that is rough on the scale of optical wavelength. The scattered yet still coherent waves interfere constructively and destructively, producing a chaotic distribution of light and dark spots [11], [12]. For the measurements of the valve kinematics the valve is equipped with a retro-reflective tape to achieve higher intensity of the backscatter light. Unfortunately, the tape itself is optically rough and still produces a speckle pattern [12], [13]. The speckle pattern is not of high significance unless it changes dynamically. Then it can translate (i.e. speckles appear to move in space while retaining their size and shape) or boil (i.e. no translation of the speckle but a continuous evolution from one size and shape to another) [16], [17]. The speckle noise is produced if the Doppler signal amplitude remains high enough for the demodulator to operate. If the Doppler signal amplitude drops to low levels and the demodulation process fails, signal drop-out occurs. During its motion the valve is designed to rotate in order to keep the valve face and seat clean of carbon deposits. This also has the effect of slightly reducing the wear [18]. Because of the acting forces the valve also experiences tilt especially at high speeds. This altogether contributes to significant speckle noise during the valve kinematics measurement and frequent drop-out noise.

Attempts have been made to define strategies for reducing the signal drop-out noise to a manageable level for industrial diagnostics [19]. Algorithms for automated identification of the presence of the signal drop-outs and the selection of an unaffected portion of data were

presented for measurements on bearings of electric motors [20]. However, the valve kinematics data are very specific so we decided to develop our own algorithm for signal drop-out recognition. To achieve this, it was first necessary to study data measured over the last 20 years to clearly identify where the drop-outs occur and to characterize them.

Since all presented figures depict data of real engines where some are still on the market, we decided not to show the real data scales but rather normalized values. As shown later, the validity of the described algorithm isn't compromised, especially because the normalization is its first step.

3.1.1 Signal drop-out during valve opening or closing

In measured data (valve displacement or velocity), one-point peaks that apparently do not form real measured values can be encountered (Fig. 3.1). They are the afore-mentioned signal drop-outs resulting from failed signal demodulation. The vibrometer controller is equipped with so-called tracking filter [21] whose purpose is to bridge those instances and improve the signal-to-noise ratio of the weak optical signal. Nevertheless, the filter has its limits. The signal drop-outs were identified while using different laser units (Polytec OFV 502 + OFV 3000, Polytec HSV 800 FF + HSV 2000) and with different measurement equipment and settings as well as in different laboratories. The better focus of the probes was performed and kept during the measurement, the less drop-outs in the measured data were encountered. The cleanness of the retro-reflective tape was also important. The size of the drop-outs ranges from short and hardly-recognizable peaks to very high and clearly visible.

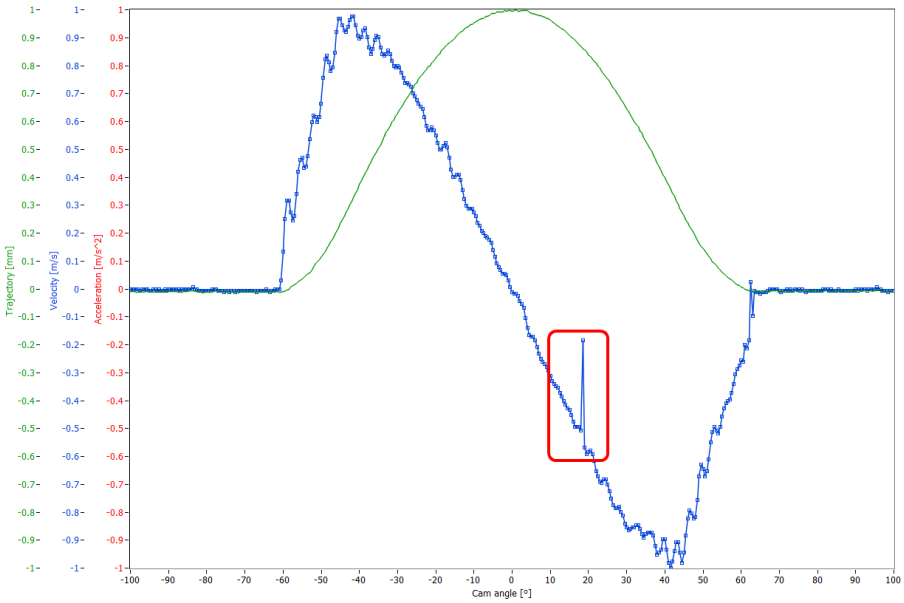

Figure 3.1 – Velocity signal drop-out

3.1.2 Base circle signal drop-out

Same principle as in *3.1.1* but it occurs on cam's base circle. It can happen in both signals. To decide whether the peak is or is not a signal drop-out largely depends on the noise level of the measured curves. The same peak if surrounded by noise would not be considered a problem. The size is significantly lower than in *3.1.1*.

3.1.3 Offset drift

Inaccurate settings of the devices can result in offset drift. When the valve is located on the base circle, the expected value of both velocity and displacement should be 0 V. Furthermore, the offset drift can be encountered due to a false reset pulse arrival. The pulse is used to reset the interferometer to assure that on the base circle the value of the measured signals will be referenced to 0 V. The IRC trigger signal is used for this purpose. The false arrival can occur due to magnetic interference from the electromotor.

3.1.4 Complete signal distortion

Resulting signal does not resemble the expected measured data. This mostly happens if focus of the probes is lost (due to vibrations or another major problem).

3.2 Localization of the phenomena

Localization of each of the named problems in the measured data is important. The parameters of the algorithm can be better targeted if we narrow the intervals for testing. This will improve accuracy and time needed for testing.

The measured data were divided (Fig. 3.2) into five intervals (*T1*-*T5*) based on the occurrence of the phenomena listed in the previous chapter. Significant endpoints were marked in the data.

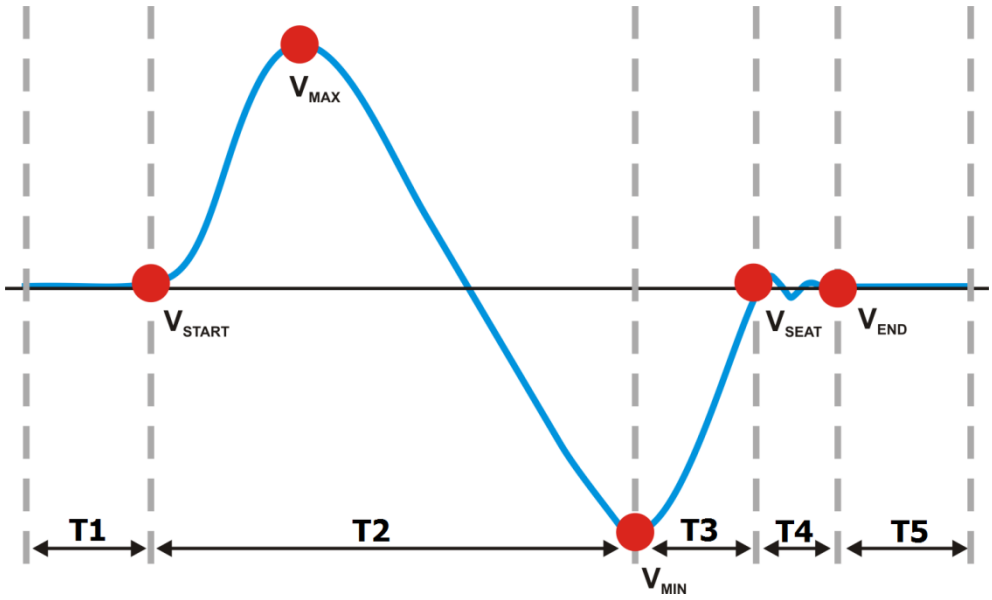

Figure 3.2 – The data intervals

Interval T1 is the portion of the signal before the valve opens. The valve is located on the base circle of the cam. In this interval offset drift of the displacement or velocity can be detected. Also the signal drop-out of both of the measured variables can occur. The left endpoint is given by the trigger pulse that starts the data acquisition. The right endpoint is the point V_{START} where the valve begins to open.

Interval T2 is the portion of the data where the occurrence of the velocity drop-out can be observed. This is the most common case and location of its occurrence. The left endpoint of this interval is the point V_{START}. The right endpoint is the minimum of the velocity (i.e. maximum during valve closing) marked V_{MIN}.

Interval T3 is very sensitive. Only its first half should be tested for the velocity signal drop-outs and the test parameters should be set to identify only drop-outs of significant size. In the second half the first contact of the valve with the seat occurs which poses a step change of the velocity and could be easily mistaken for the signal drop-out. A typical example would be a valvetrain with worn valve guides. In such a situation the algorithm would re-start the measurement, thus eliminating the possibility to discover the malfunction of the valvetrain. The second half of *T3* could be used in the future for detailed study of automatic determination of the impact velocity, which is a crucial parameter for the valvetrain lifetime.

Intervals T2+T3 together form interval where the test for detection of displacement signal drop-outs should be applied. In this case the test can be applied also to *T3* since the valve's first contact is not detectable from the displacement curve and thus cannot be mistaken with the signal drop-out. The right endpoint V_{SEAT} is a theoretical point where the valve fully sits for the first time in the seat. As will be shown later, this point is easily determinable.

Intervals T4+T5 together should be used for detection of the displacement offset drift and displacement drop-out. The left endpoint is V_{SEAT} and the right is the end of the data record.

Interval T5 is used for the velocity offset drift detection and the velocity signal drop-out detection. *Interval T4* is not tested, since there the valve can still oscillate with step changes in velocity. The left endpoint is given by point V_{END} which marks the point where the valve does not oscillate anymore (the valve is on the cam base circle and does not bounce).

These intervals denote portions of data that will be introduced to particular tests. As mentioned earlier, the velocity and displacement of the valve are measured. For separation into the described intervals, the velocity curve is used. It is not possible to separate the measured data into meaningful intervals based on the displacement curve, since the changes in displacement are too small and do not allow for clear identification of each phase of the valve cycle. It is not possible to use the acceleration either. It is obtained as finite differences from the velocity and has very noisy character. Multipoint difference methods could be used or smoothing of the signals could be applied. However, since different noise levels are present across the measurements and different pprs are often utilized, it would be difficult to create a smoothing algorithm suitable for every condition.

3.3 Separation

It is crucial for further processing to precisely identify the intervals' endpoints. It is not a trivial task since their determination can already be influenced by the existence of phenomena like offset drift or signal drop-out. Different resolutions of the data acquisition that can be used also play a role.

The first step to successfully determine those points is to normalize the acquired data. A normalization that provides a unified range of values for our algorithm has to be chosen. This is because the shape of the measured curves can vary significantly across different valvetrains, as can the absolute values across different speeds. The key seems to be the *normalization to "1"*. V_{MAX} and $abs(V_{MIN})$ are identified in the velocity data. The higher of those two is chosen and the whole dataset is divided by this value. This way the velocity in the range of -1 to 1 m/s is obtained.

During the measurement, five continuous datasets for each engine speed are acquired. Each dataset is independently analyzed and V_{START}, V_{MAX}, V_{MIN}, $V_{SEAT,}$ V_{END} for each of

them is determined. Then the median value is taken, thus filtering out extreme values and obtaining coordinates of each endpoint for a particular engine speed.

V_{MIN}, V_{MAX} – these two points are easily detectable. They are the maximum, respectively minimum (maximal velocity during valve closing) of the velocity.

V_{START} – is the point where the valve begins to open. It is important to realize that a simple condition such as: "*We look for a point where successive N points lie above zero value*" won't be enough. This approach fails if the velocity has drifted offset and it will find false index. For our purposes following definition seems to work quite well: "*We look for an index where all points between this index and the velocity maximum have a value higher than the value of the point on that index."*

The second necessary condition utilizes a simple outlier test [22]. Such a point and the following 3 points (generally *p1* points, where *p1* is a parameter of the algorithm) has to have the deviation from the mean of all the preceding points at least 3 times (generally p_2 times, where p_2 is a parameter of the algorithm) higher than the standard deviation ('three-sigma' rule [23]) of the preceding values. In other words, point where the curve starts to rise steeply is found, e.g. the point where the cam profile changes from the base circle.

In summary:

We take the values of velocity $v_1 \dots v_{MAX}$ *and we look for* v_i *so*

i. $v_i < v_j \; where \; j = i+1, \; i+2, \dots MAX$

ii. $\sigma_{i-1} < p_2 \cdot s_k \; where \; k = i+1, \; i+2, \dots p_1; \; s_k = \sqrt{(v_k - \bar{v}_{i-1})^2}$

$\bar{v}_{i-1}$ *is the mean of the preceding values* $v_1 \dots v_{i-1}$ *and* σ_{i-1} *their standard deviation.*

V_{SEAT} – is the point where the valve reaches the seat the first time. Especially with high engine speed the valve can bounce a few times [6] or oscillate before it fully closes and remains on the base circle of the cam. Such a point is easily detectable by examining the data of the velocity from the V_{MIN} index to the end of the dataset. We attempt to find a point that has a value higher than the mean of the rest of the consecutive data, e.g:

We take the values of velocity $v_{MIN} \dots v_m$ *and we look for* v_l *so* $v_l > \bar{v}_{l+1}$ *where* $\bar{v}_{l+1}$ *is the mean of the values* $v_{l+1} \dots v_m$

V_{END} – is the point where the bouncing of the valve (if present) disappears and the valve fully follows the cam base circle profile. The ideal situation would be V_{END} = V_{SEAT} which would mean the valve smoothly closed without bouncing. The data from the index of V_{SEAT} to the end of the record are taken. The mean of this portion is calculated and the oscillations are then analyzed. The highest value (amplitude) of each part above and below the mean level is determined.

The average amplitude of the oscillations $\bar{a}$ is calculated. The algorithm then looks for p_3 consecutive sequences that have the amplitude less than the given threshold. Parameter p_3 is dependent on the measurement ppr. For example for ppr = 720 it looks for 4 consecutive sequences meeting the criteria. Every additional 1800 ppr raises the number by 2. The threshold is set as p_4 times $\bar{a}$. If the calculated threshold is higher than parameter p_5, p_5 is used instead. This can happen if the dataset ends before the oscillations disappear (usually if the DAQ was started too early on the base circle right after the valve closed).

3.4 Tests

Tests to automatically recognize the signal drop-outs in the above described intervals were developed. The tests have to be accurate and robust at the same time. This will assure that the tests won't fail even with very special valvetrain designs, such as racing valvetrains. At the same time the tests have to be able to distinguish between the phenomenon and the real trait of the valvetrain. Let's assume a situation that the examined valvetrain has a malfunction that appears only once in a while. If the tests weren't designed accordingly they could identify the malfunction as the signal drop-out. They would repeat the measurement until they'd get a satisfactory result. This way the engineers would never realize that the valvetrain deserves a detailed investigation.

The test of the velocity signal drop-out recognition for *Interval T2* will now be described, along with the process used to achieve its final state. The other signal drop-out tests are merely a variation with slightly different parameters.

3.4.1 Signal drop-out test

Three techniques were compared. Since the signal drop-out peak always consists of only one point, the first technique used was to calculate the distance from the center of the two points on the sides. This way, a graph of extremes on the baseline was obtained. The second approach was to utilize the Discrete Wavelet Transform (DWT). The first level of the *detail coefficients* was used to recover the high frequency portion of the data. Different types of wavelets were tested. The *db03* wavelet (which is asymmetric, sharp, irregular and resembles the shape of the peak) seems to show the best results. The third approach was to use a highpass digital FIR filter designed for our purposes. The Parks-McClellan [24] algorithm (SB=200Hz, PB=4000Hz) was used to obtain the filter coefficients. Since each filter has some start-up time, it was necessary to avoid the artifacts at the beginning and at the end. The data were symmetrically appended by reversing the needed amount of samples (which equals the order of the filter) at the beginning and the end. The data were then filtered for the first time. The filter parameters were set as if the data were sampled with constant frequency F_s=10 kHz. This way, universal settings for filtering out the baseline could be set (the cutoff frequency SB/LB won't change with different ppr and the amount of samples in the interval under examination). Then the data were reversed and filtered again with the same settings. This way the shift introduced by the filter was removed. In the end the data were reversed back and the data portion that was appended to the beginning and the end was deleted. The absolute value of the resulting signal was taken in order to clearly show the peaks.

From those three techniques the custom FIR filter approach was chosen. It delivers the best results and the best signal-to-noise ratio (SNR) even for small peaks as can be seen in (Fig. 3.3)

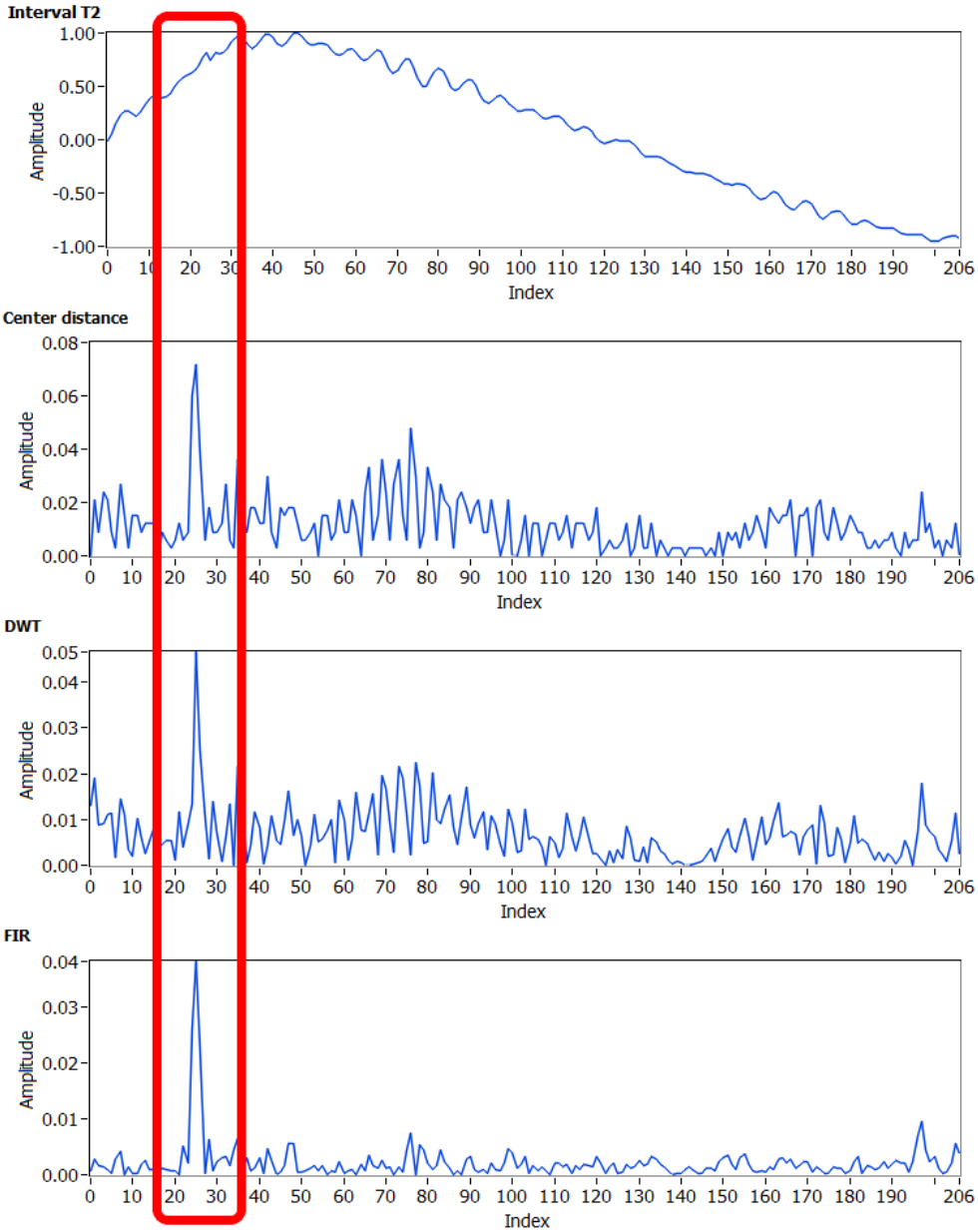

Figure 3.3 – Different techniques of signal drop-out detection; small peak

Now the signal (which may or may not contain drop-outs) is available. The next step is to recognize whether it was affected by the phenomenon. Simple thresholding would not be sufficient. The same peak which can be considered drop-out in one dataset would not meet the criteria in another. What distinguishes them is the level of surrounding noise. This situation is clearly visible in Fig. 3.4. In the top picture the peak reaches the value 0.04 and should be marked as signal drop-out. In the bottom picture the same value would not be considered a signal drop-out. The red line shows the estimated noise level.

If the noise level of the signal can be determined, the SNR of the data can be calculated by dividing the value of the top of the highest peak (h) by the noise level (n). The SNR has become the criterion which decides whether the measurement should be restarted.

$$SNR = \frac{h}{n} < c \qquad \text{where } c \text{ is the criterion.} \tag{9.1}$$

If SNR > c than the signal should be re-measured.

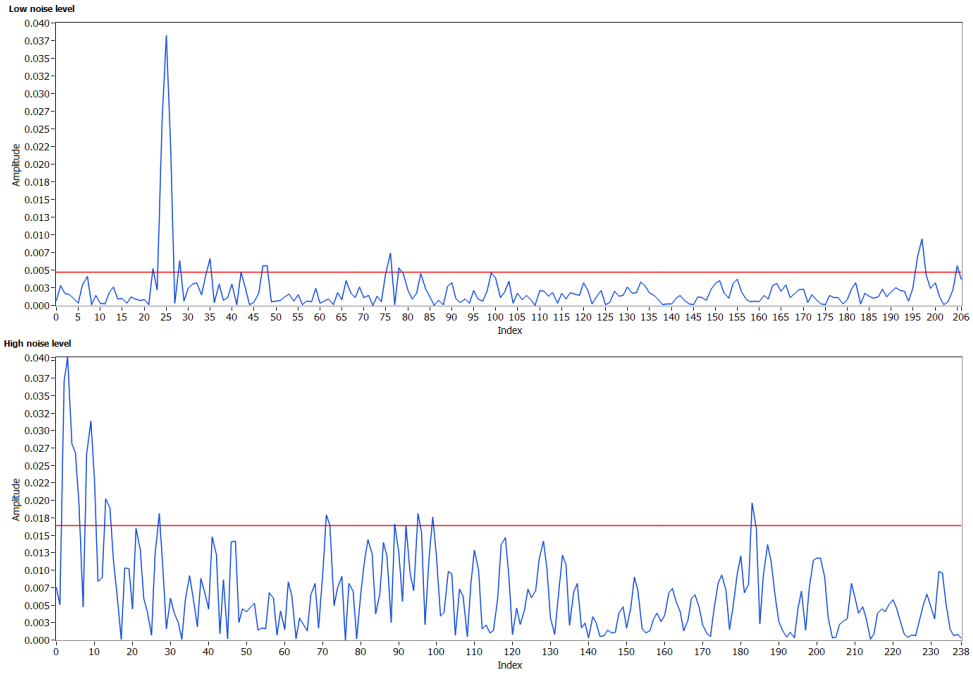

Figure 3.4 – Comparison of low noise level and high noise level

To determine the noise level a statistical approach was adopted. Our data after filtration consist mostly of peaks of speckle noise that was superimposed on the baseline. The occurrence of the signal drop-outs in one dataset is not high (usually one peak in one dataset). The occurrence of multiple drop-outs is quite rare.

First the peaks are sorted in ascending order by their size. Then the peak that is at 85% of the total count of the peaks is selected (in other words the 85th percentile). Its value determines the noise level. This approach is possible since the drop-out peaks will always be among the highest 15%. Fig. 3.5 shows the described procedure with the peak shown in Fig. 3.3.

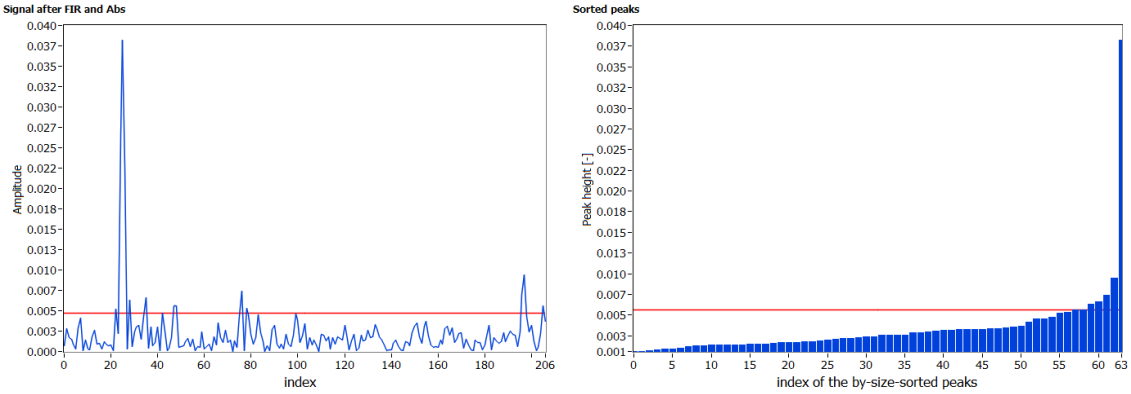

Figure 3.5 – Peak sorting and 85% noise level estimation

The parameters of this algorithm are then the percentage used to determine the noise level (*p6*), the SNR criterion *c (p7)* and also the minimal size of the drop-out peak h_{min} *(p8)*. For the velocity signal drop-out detection algorithm for *Interval T2* the parameters after

testing were set as $p_6 = 85\%$, $p_7 = 4.5$, $p_8 = 0.01$. In other words, to mark the dataset under investigation as affected by the drop-out phenomenon, it has to have the SNR of 4.5 or higher and the highest peak has to be higher than 0.01. The noise level is obtained by taking the value of the 85% peak.

To keep the robustness of the detection algorithm, an additional evaluation of the provided results was implemented. If the algorithm marks more than half of the datasets taken at the same engine speed as faulty, the evaluation algorithm will check the positions of the detected peaks. If the positions of the drop-outs are the same (or nearly the same) then the signal is saved so the engineer can decide whether the data are showing a trait of the valvetrain or just a drop-out. The p_9 parameter of the algorithm is the allowed peak index position difference. It is expressed as the percentage of ppr.

4 Comparison of measured data of two different valvetrains

To verify the capabilities of the constructed system, a series of measurements was carried out. First the standard 1.2 HTP OHC valvetrain in the half-engine setup was measured. Then it was replaced with a low friction version of the valvetrain and measured again. The low-friction type has thinner springs with smaller stiffness; the cam lobes are thinner as is the cam follower to achieve smaller contact area and less mass. Different materials and bearings are used to achieve smaller rolling friction. The valves are the same in both cases.

All the measurements, unless stated otherwise, were carried out from 1000 rpm to 5000 rpm with an increment of 1000 rpm and from 5100 to 6000 with 100 rpm increment. Five consecutive periods of the measured variables were always stored. If the signal drop-out was recognized, the data were re-measured. The IRC ppr was set to 720 offering resolution of 0.5° of the cam. The measurements were not started before a 15-minute warm up procedure in which the oil temperature reached at least 40 °C.

Since the figures presented in the following text depict data characterizing real valvetrains that are on the market, we decided to withhold the real data scales of the kinematic variables. The *"1" normalized* values (data rescaled to range from -1 to 1) are shown instead. This approach does not compromise the validity of the data since the purpose is to carry out the comparison of the variables of the two valvetrains.

4.1 Measurement time duration

One of the main motivations for the development of this automated system was to reduce the duration of the measurement. The comparison of the measurement times can be found in Table 4.1. The times show the duration of the measurement procedure of one valve. The measurement procedure was always repeated 10 times, with the average time calculated. The time saving of the developed automated system is apparent. However, it is even more important that the application saves data that are not affected by the drop-out phenomenon and thus does not demand additional processing before performing the standard analyses.

Table 4.1 – Measurement duration results

	Average duration of the measurement procedure (15 data sets, 1000 rpm to 6000 rpm)
Original system manual slip correction, visual data testing, manual data saving	cca 10 min (reported by the test engineers of ŠKODA AUTO a.s)
Developed automated system slip correction ON: ± 5 rpm; data testing ON	2:25 min (in average 5 data files were re-measured because signal drop-out or other phenomenon was recognized)
Developed automated system slip correction OFF; data testing OFF	1:29 min

4.2 Camshaft speed fluctuations across the whole engine speed spectrum

One of the beneficial analyses which can be carried out thanks to our complex system is the analysis of the camshaft speed fluctuations across the whole spectrum of the operational engine speeds. Information about the percentage deviation of the camshaft speed from its average value at a given engine (crankshaft) speed can be obtained. For this reason we carried out the measurement from 300 rpm to 6000 rpm with a 100 rpm step.

The following figures show the dependency of the maximal negative deviation from the average camshaft rpm (- *deviation*, red dashed-dotted line) on the engine rpm expresses as percentage of the actual speed. The green dotted line (+ *deviation*) denotes the maximal positive deviation. The black solid line is the mean of those two. Fig 4.1 shows those values for the intake and the exhaust camshafts of the standard 1.2 HTP engine valvetrain together with 3^{rd}, 6^{th}, 9^{th} and 12^{th} order of the base (camshaft) frequency. Fig 4.2 depicts the same for the low-friction valvetrain. The values from 300 to 500 rpm show high deviation which is not caused by the combustion engine but by the driving electromotor. At such a low speed the electromotor cannot ensure driving at a constant speed due to the variation of the torque during one revolution of the crankshaft. The inertia of the moving parts doesn't help to smooth the motion and allow the electromotor to revolve with a constant torque (thus a constant driving speed).

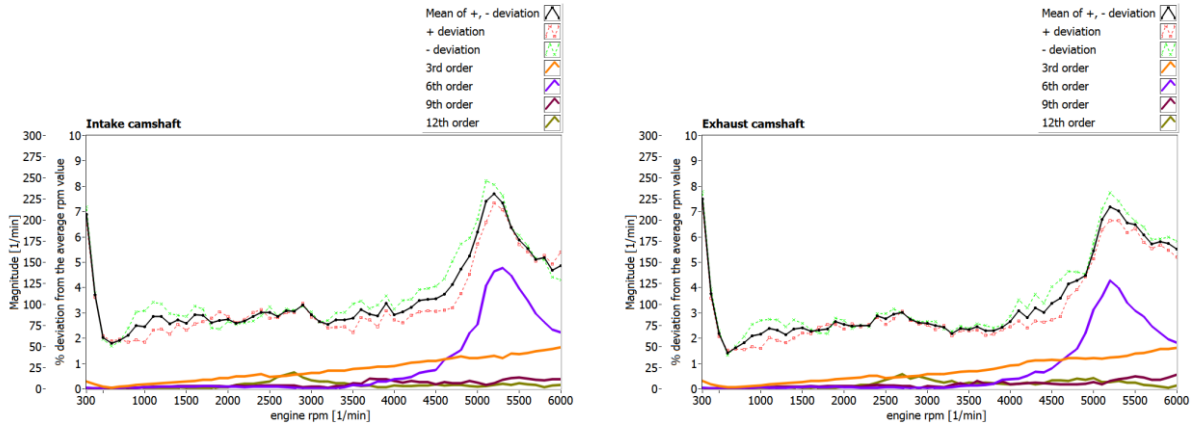

Figure 4.1 – Percentual deviation from the average rpm value and the orders of base camshaft frequency across the whole engine operational spectrum, *standard* 1.2 HTP valvetrain, half-engine setup

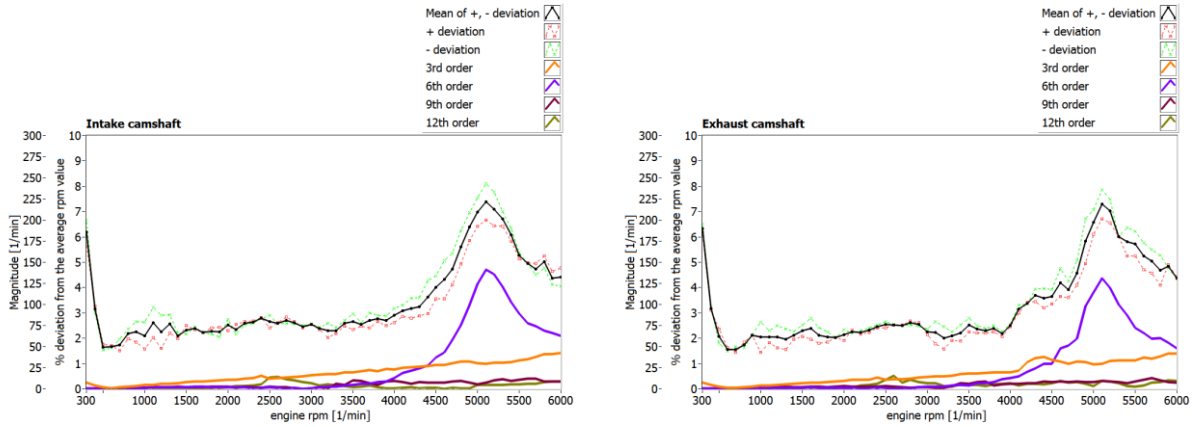

Figure 4.2 – Percentual deviation from the average rpm value and the orders of base camshaft frequency across the whole engine operational spectrum, *low-friction* 1.2 HTP valvetrain, half-engine setup

The deviation has a clear rising trend with its peak around 5100 rpm. The peak is presumably caused by the resonance of the timing chain (resonance of 6th order; 255 Hz). The other possibility is the resonance of the chain tensioner blade. To discover the true origin, additional experiments would have to be carried out. The plastic tensioner blade could be exchanged by a more rigid type, and the fluctuations remeasured. As expected, after passing this critical frequency the deviations begin to drop. The same trend can be seen in both the intake and the exhaust camshaft data of both the standard and the low-friction valvetrain. Both of the valvetrains show approximately the same level of speed fluctuations across the measured speeds.

4.3 Computation of valve acceleration using the speed fluctuation information

Valve displacement and velocity are measured. However, from the point of dynamics and verification of the proper function of a valvetrain, the most valuable source of information is acceleration. The most common approach is to obtain it from the measured velocity using a numerical derivative. The reason is that it is complicated to obtain acceleration of a valve directly, accurately, and reliably at a high rpm. A piezoelectric accelerometer can be difficult to attach to the valve and its mass influences the resulting data. Special low-weight (1 gram) accelerometers can be purchased but even then the problems with connecting cables that tend to separate at high rpm persist. Nevertheless, there were some attempts made usually at low speeds and with the accelerometers attached to various parts of the valvetrain components [25], [26], [27], [28]. Since the high speed laser Doppler vibrometers became the standard device for measuring the kinematics of the valves, acceleration has been obtained indirectly from the velocity [6].

In order to obtain acceleration, we usually utilize either a forward or backward numerical derivative. The reason is that these simple methods reveal step changes in the velocity signal (for example, the first contact of the valve with the seating [7]). The advanced methods tend to smooth the data so these phenomena would remain unnoticed.

It is important to mention that the measured signal is sampled with respect to the cam angle, and not the time. Thus, the time derivative is not an option. If we want to obtain acceleration, we have to use the following approach:

$$\omega = \frac{d\varphi}{dt} \tag{4.1}$$

$$a = \frac{dv}{dt} \quad \text{if we use the equation (4.1) we get} \quad a = \frac{dv}{d\varphi} \cdot \omega \tag{4.2}$$

Using the numerical differences it can be written as

$$a = \frac{\Delta v}{\Delta \varphi} \cdot \omega \tag{4.3}$$

If we neglect the accuracy of the IRC the angle difference will be constant. Expressed in radians:

$$\Delta\varphi[rad] = \Delta\varphi[deg] \cdot \frac{\pi}{180}; \qquad \Delta\varphi[deg] = \frac{360}{ppr}; \quad \rightarrow \quad \Delta\varphi[rad] = \frac{2\pi}{ppr}; \tag{4.4}$$

The camshaft angular velocity is

$$\omega = 2\pi f_{cam} = \frac{2\pi\, rpm_{cam}}{60} \tag{4.5}$$

Using the equations (4.4) and (4.5) in (4.3) we have

$$a = \frac{\Delta v\, rpm_{cam}\, ppr}{60} \tag{4.6}$$

Common practice is to neglect the variance in rpm_{cam} and presume the rotational speed to be constant. The main reason is that synchronized information about camshaft speed fluctuations is not usually available. Let us consider the measured data in Fig. 4.3 where the valve velocity is synchronized with the camshaft speed. The speed of 5100 rpm was chosen because the highest deviation from the average of the speed was encountered at this speed.

In Fig 4.4 we can see the comparison of the acceleration calculated while presuming a constant camshaft speed (black) and the approach that gets the benefit of the measured speed fluctuations (red). The formula (4.6) and the forward finite difference were used.

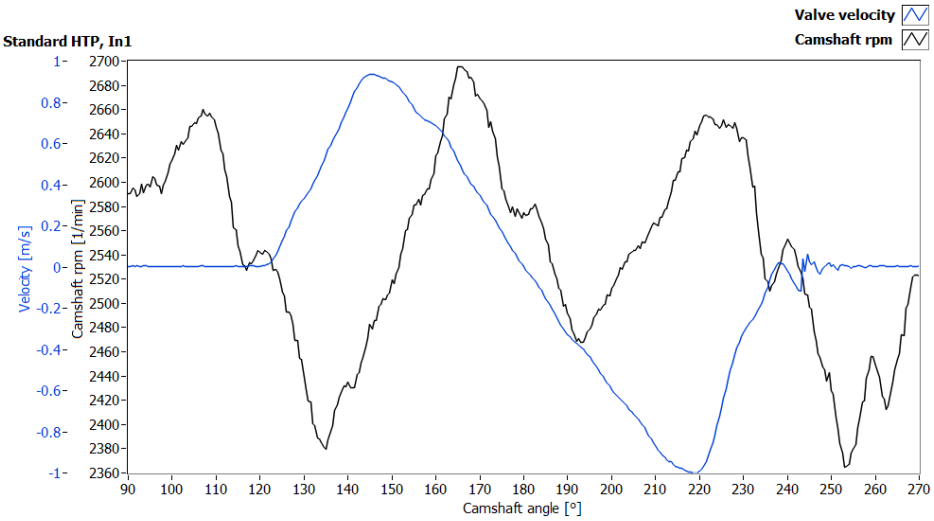

Figure 4.3 – Valve velocity and camshaft speed, *standard* 1.2 HTP valvetrain, In_1, rpm_{crank} = 5100

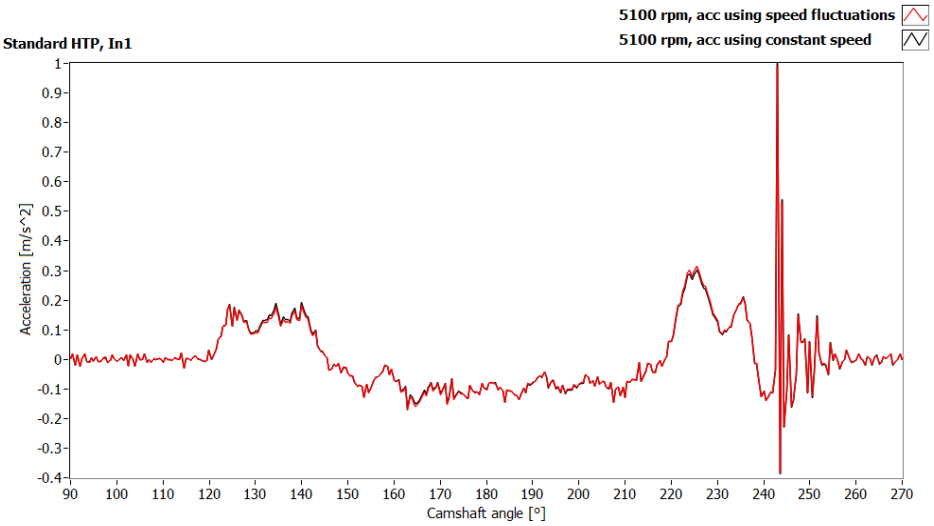

Figure 4.4 – Calculated acceleration of the valve, rpm_{crank} = 5100, In_1, forward difference, half-engine setup

Only slight differences between the calculated curves can be observed. It is safe to say that in the case of modern valvetrains, rotational irregularities do not play a significant role in the valve acceleration calculation and the rotation can be simplified as constant for this purpose.

5 Comparison of measured values of valvetrain in half-engine setup and partial-engine setup

In industry, the measurement of kinematic variables of OHC valvetrains is usually simplified. Rather than testing the complete engine, assembly of merely the head and head cover is used. We will call it *partial-engine setup* in the following text. Such a setup is easy to assemble, and does not demand additional modifications of the components while, at the same time the exchange of the valvetrain components is fast and the valves are easily optically accessible.

The *half-engine setup*, in contrast, uses nearly a complete engine. It requires the pistons to be removed and the crankshaft replaced by a straight dummy shaft. Apertures have to be milled in place where the pistons belong in order to allow access of the laser Doppler probes to the valves. The timing chain cover has to be modified to allow attachment of the IRC sensor. The engine is attached to a rigid test frame and driven by an electromotor. The half-engine setup is as close as possible to the real engine assembly which is mounted in an automobile.

Since preparation of the half-engine setup is time-consuming, the simplified setup is preferred. Our partial-engine setup (see Figure 5.1) consists of a rigid steel plate holding the apparatus. Two supports are attached to the plate, upon which the cylinder head and the cover are mounted. A head gasket separates the cylinder head from the supports and prevents oil leaks. One support has a channel for pressurized oil distribution since the engine's oil pump and distribution channels are not present (normally the oil is brought through the engine block). The engine oil pump is replaced by an external oil unit and distribution system. The oil from the head is collected through the oil outlets of the cylinder head. A custom side cover was manufactured to replace the missing timing chain cover, and a pulley is mounted at the end of the driven camshaft. The torque transfer between the driving electromotor and the pulley is assured by a ribbed belt. The IRC sensor is attached to the pulley to offer precise information about the position and speed of the camshaft.

Such a setup poses only a fraction of the original mass of the engine. Nevertheless, it is expected to deliver results close to the half-engine setup and thus close to the values of a real operating engine [15]. Although the partial setup has become a widely-used solution since the OHC valvetrains became standard, no direct comparison of the same valvetrain in half-engine and partial-engine setup has been published (to the author's knowledge). We conducted this comparison on a 3-cylinder ŠKODA 1.2 HTP engine – first with a standard valvetrain and then with its low-friction version. The main focus was on the valve kinematic variables, but the two setups were also compared from the point of camshaft speed fluctuations. The IRC ppr was set to 720 offering resolution of 0.5° of the cam.

Since the figures presented in the following text depict data which characterize real valvetrains that are on the market, we decided to withhold the real data scales of the kinematic variables. The normalized (*"1" normalization* – normalized values in range from -1 to 1) values are shown instead. This approach does not compromise the validity of the data since the purpose is to carry out a comparison of the variables.

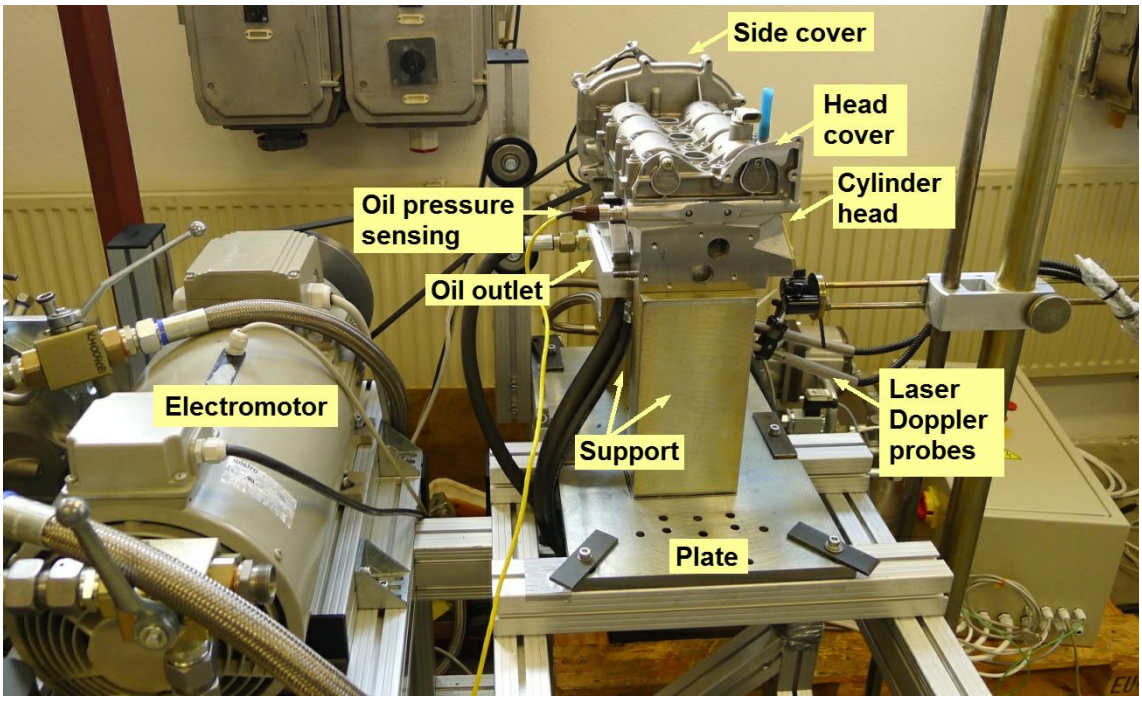

Figure 5.1 – Engine in partial setup

5.1 Camshaft speed fluctuations across the whole engine speed spectrum

Speed fluctuations of the partial-engine setup were expected to be significantly different from the half-engine setup. This is a result of missing moving parts and driving of only one camshaft at a time. The camshaft speed fluctuations of the partial-engine setup are caused mainly by the shape of the cams of the driven camshaft and the springs' force. The stiffness, length, tension and alignment of the belt that is used to drive the camshaft also play a significant role.

The following figures show the dependency of the maximal deviation from the average camshaft rpm on the engine rpm expresses as percentage of the actual speed. Fig 5.2 shows those values for the intake and the exhaust camshafts of the standard 1.2 HTP engine valvetrain in the partial setup together with 3rd, 6th, 9th and 12th order of the base (camshaft) frequency. Fig 5.3 depicts the same for the low-friction valvetrain. The same analysis for the half-engine setup can be seen in Fig 4.1 and Fig 4.2. The corresponding discussion can be found in chapter *4.2 Camshaft speed fluctuations across the whole engine speed spectrum*. Direct comparison is depicted in Fig 5.4 and 5.5.

The measurement was carried out from rpm_{crank} = 1000 rpm with 100 rpm increment. Uniform rotation of the driving electromotor was not achievable at lower speeds (< 1000 rpm) due to the variation of the torque during one revolution of the camshaft.

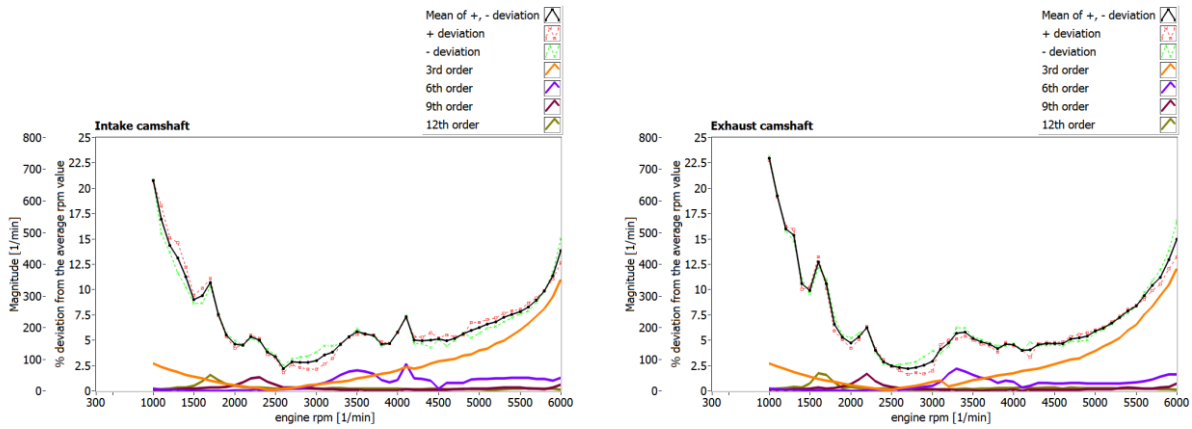

Figure 5.2 – Percentual deviation from the average rpm value and the orders of base camshaft frequency across the whole engine operational spectrum, *standard* 1.2 HTP valvetrain, partial-engine setup

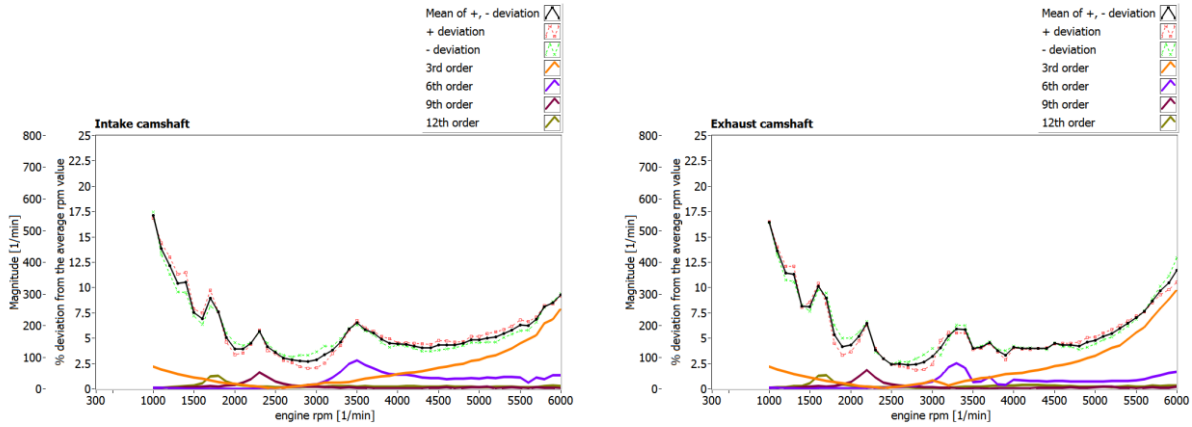

Figure 5.3 – Percentual deviation from the average rpm value and the orders of base camshaft frequency across the whole engine operational spectrum, *low-friction* 1.2 HTP valvetrain, partial-engine setup

At first the deviation has decreasing tendency up to 2500 rpm. With increasing speed the inertia forces increase and help to smooth the motion of the camshaft. Local maxima can be identified in the data. They are caused by the resonances of the strands of the belt (belt connecting the electromotor and the camshaft). Some of them were even clearly observed during the measurement, e.g. local maximum around 3500 rpm (resonance of 6^{th} order). The belt resonance primarily occurs when the natural frequency of some length of the belt is excited by a frequency generated by the drive.

From 4500 rpm the percentual deviation begins to steeply rise again. The exact origin has not been identified. It would be interesting to carry out the measurement over 6000 rpm to discover where the resonance occurs, if it indeed does. Another option would be to repeat the measurement with a shorter and more rigid belt and observe the change in the trend. This would reveal if the resonance of the belt is involved. The last possible (but unprobable) explanation of the increasing speed fluctuation would be increasing torsional vibrations in the camshaft. To verify this theory, we would have to alter the moment of inertia of the camshaft; for example by adding metal rings and repeating the measurement.

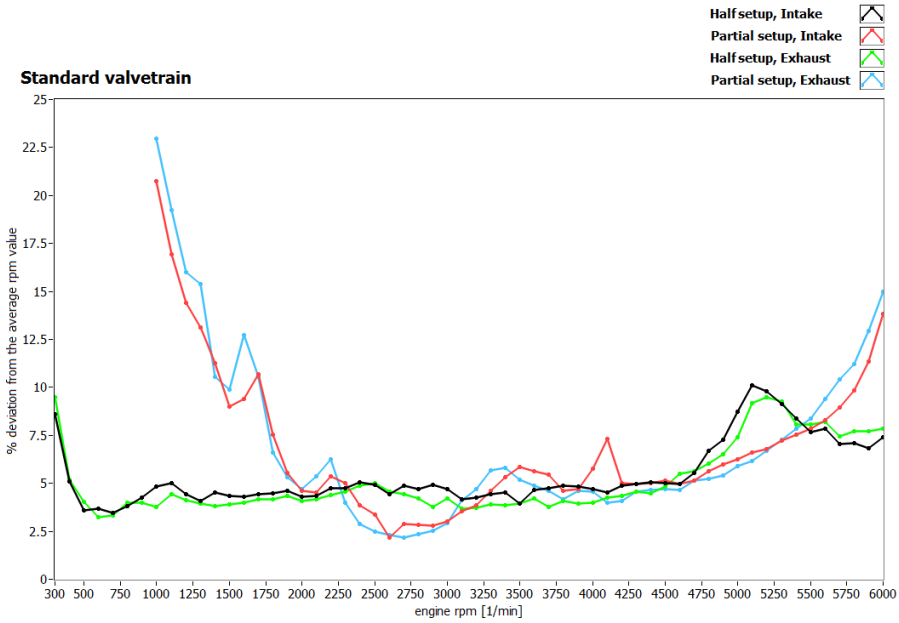

Figure 5.4 – Mean percentual deviation from the average rpm value across the whole engine operational spectrum, *standard* valvetrain, comparison of partial and half-engine setup

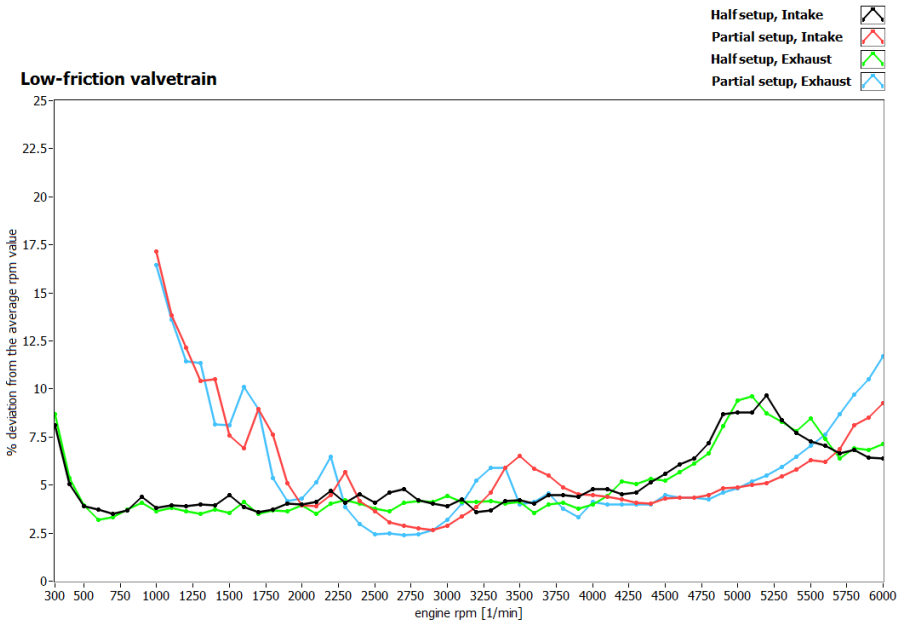

Figure 5.5 – Mean percentual deviation from the average rpm value across the whole engine operational spectrum, *low-friction* valvetrain, comparison of partial and half-engine setup

It can be concluded that the camshaft speed fluctuations significantly differ between the half-engine and the partial-engine setup at different speeds. The profound difference up to 2000 rpm is caused by the absence of the crankshaft and the second camshaft in the partial-

engine setup. The inertia of the shafts and the counter torque of the cam lobes of the second camshaft help to smooth the rotation of the half-engine setup at a low speed. The differences with increasing speed are the result of resonances of different parts of the systems.

Nevertheless, these results were expected based on the differences of the two setups. It would be interesting to compare the measured data with the measurements of the partial-engine setup with both sprockets driven, contributing with the rotational irregularity of both camshafts. Such a system would be closer to the half-engine setup but would demand additional changes.

5.2 Direct comparison of the speed fluctuations

The differences in the speed fluctuations between the half-engine and the partial engine setup seem to be the key for understanding the differences in the measured valve kinematic variables.

The following figures (Fig 5.6 and 5.7) depict the speed fluctuations and how they change with the speed of the engine. The frequency of the camshaft sprocket-teeth (36 teeth) can be identified in the measured data of the half-engine setup at 1000 rpm. With increasing speed (starting at 4500 rpm) the 6th order of the camshaft base frequency becomes dominant in the data of the half-engine setup (in detail in the thesis itself). In the partial-engine data the magnitude of the 3rd order becomes dominant at 4000 rpm (see also Figures 5.2 and 5.3 for detail). Also a phase shift of the oscillations with increasing frequency can be recognized. This is clearly visible in the following figures, especially in the data of the partial-engine setup between 1000 rpm and 2500 rpm.

To identify the exact origin of the differences in the speed fluctuations (amplitude, phase, orders) between the two setups we would need precise numerical models. To construct them is beyond the scope of this thesis and leaves door open for future research.

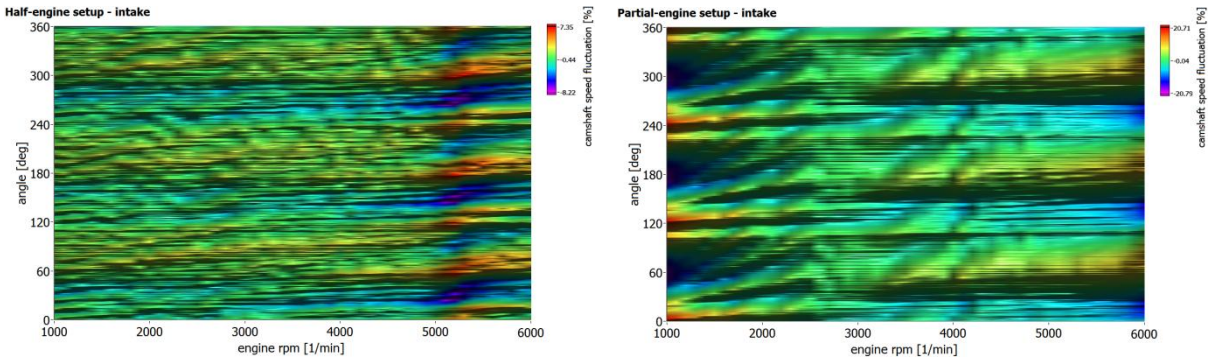

Figure 5.6 – Speed fluctuations, *standard* valvetrain, *Intake* camshaft, comparison of half (left) and partial (right) engine setup

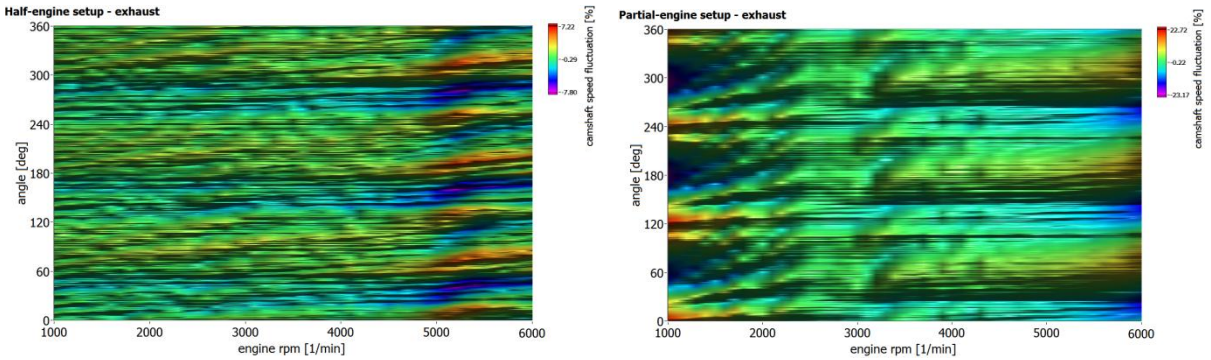

Figure 5.7 – Speed fluctuations, *standard* valvetrain, *Exhaust* camshaft, comparison of half (left) and partial (right) engine setup

5.3 Comparison of the kinematic variables

The most important comparison and reason why we carried out these measurements is the comparison of the kinematic variables. The question posed was whether the partial-engine setup delivered the same values of kinematic variables as the half-engine setup, i.e. whether the change in the speed fluctuations and missing parts of the valvetrain significantly change the valve behavior.

Figure 5.8 depicts the comparison of the valve kinematic variables of the first intake valve (closest to the drive, In_1) of the standard valvetrain. The values of the last intake valve together with the values of the low-friction valvetrain are presented in the thesis itself.

The acceleration was calculated using the central-difference formula of the 4th order that helps suppress the influence of the noise in this case:

$$f' = \frac{-f(x+2h)+8(x+h)-8(x-h)+f(x-2h)}{12h} \tag{11.1}$$

No difference of the valve displacement curves was noticed. Only small random offset drifts caused by resetting the laser probes and different levels of noise can be traced in the valve displacement data. There are noticeable differences in the maxima of the valve velocity, which are caused by differences in the speed of rotation of each system and are explained in the thesis.

It can be concluded that in most cases, the measured variables of the partial-engine setup are fairly close to the variables of the half setup. However, there are some cases where the legitimacy of usage of the partial-engine system could be questioned, especially from the point of the valve acceleration. An example could be the data of In_1 at 6000 rpm (Fig 5.8). In this case, the half setup has a significantly higher amplitude of acceleration oscillations than what would be measured by the partial-engine setup. These data could lead to false conclusions about the necessary stiffness of the cam springs or behavior of the valvetrain. These differences are noticeable from approximately 5700 rpm and are most likely a result of the difference in the speed fluctuations between the two setups that continue increasing from 5500 rpm.

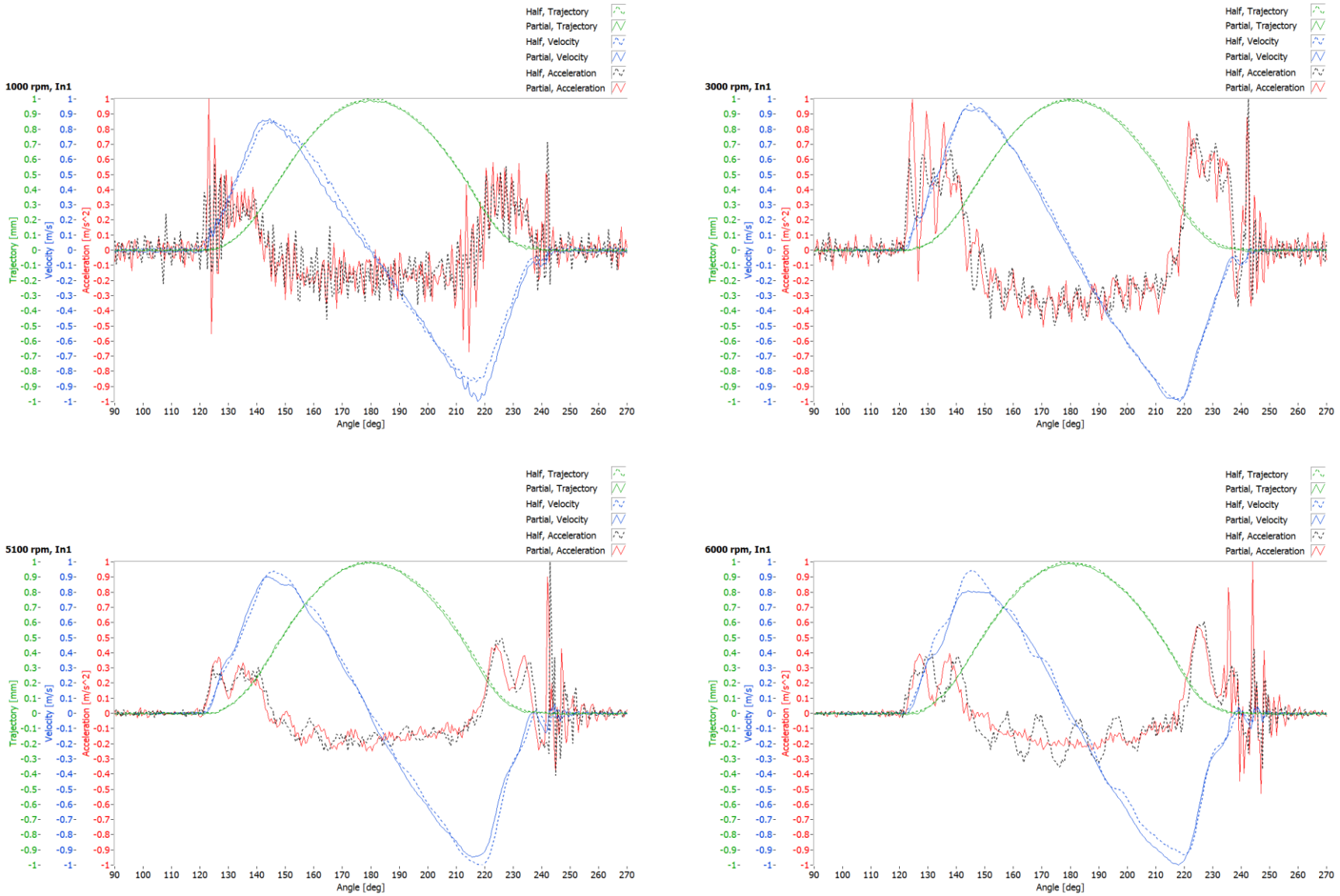

Figure 5.8 – *Standard* valvetrain, In_1, Comparison of valve kinematics of half-engine setup (dashed lines) and partial-engine setup (solid lines)

6 Summary and discussion

The current measurement procedure of valve kinematics is time-consuming. The measurements are carried out over the given operational spectrum of the engine rpm. Higher frequencies tend to be more interesting for further processing, and thus are measured in detail with smaller rpm increment. At the same time it is necessary to have high throughput of the testbed. The aim of this work was to design, construct, and test a new generation of the apparatus for valve kinematics measurements, and to overcome the limitations of the current systems (namely time consumption, high level of manual tasks which could be automated, and saving of data affected by drop-out phenomenon).

At the beginning of this project, a multipurpose automated apparatus was constructed and has been improved in the last four years. Like the previous systems, it takes advantage of the non-contact nature of high-speed Laser Doppler Vibrometry (LDV) which has become a standard measurement technique for obtaining the displacement, velocity and acceleration of the valves. The designed apparatus spans all of the engine's operational speeds and can operate a half-engine or a partial-engine setup (the latter which utilizes only the head and the head cover and the related valvetrain components). The control software (developed in LabVIEW) automatically compensates for slippage of the ribbed belt that is used to transfer the torque between the shaft of the electromotor and the combustion engine. Moreover, it is capable of a truly parallel measurement of camshaft speed fluctuations, which helps to verify the proper function of the valvetrain components. Most of all, with the algorithm for LDV drop-out noise detection, the system is fully automated. It runs the measurement across predefined engine speeds, repeating if drop-out noise is detected and saving only the representative data for further processing.

During the first development stage two communication protocols for driving the electromotor were implemented: Siemens USS protocol and Lenze LECOM protocol. Motivation for the creation of the USS protocol API was the nonexistence of any implementation of the protocol into LabVIEW. As both developed libraries were given for public use, other users had already reported their usability. The resulting automated application now benefits from the implementation of both protocols, supporting a wide palette of different controllers which drive the engine through the connected electromotor.

A detail study of the available frequency measurement methods which utilize the counters of programmable counter boards was carried out. *Method 1 – Inverse period measurement* was selected for measurements where IRC pulse per revolution (ppr) is set to 720. For higher frequencies, e.g. for ppr = 3600, we selected *Method 3 – Measure time of known number of cycles* with divider = 4. Method 1 (M1) offers the frequency measurement error of 0.03% and Method 3 (M3) of 0.04% (at rpm = 4500). The application dynamically switches between the two if needed. We carried out tests to measure speed fluctuations of revolving shafts and discovered the precision of the IRC sensor to be the limiting factor for the overall accuracy. The worst error of the one-speed sample reading (between two consecutive IRC pulses) given by the accuracy of the IRC is 4% with M1 and ppr = 720 and 5% with M3 and ppr = 3600. We also outlined the half-width size of the moving average filter for both the methods to improve the measured results: M1 = 3 samples per 720 samples; M3 = 4 samples per 3600 samples and divider 4.

The main problems which arise during automation of the LDV measurement are *speckle noise* and *signal drop-outs.* A speckle pattern is produced when the coherent waves of the incident laser beam are dephased during backscatter from a surface that is rough on the scale of optical wavelength. The scattered yet still coherent waves interfere constructively and destructively, producing a chaotic distribution of light and dark spots. The speckle pattern is

not of high significance unless it changes dynamically. It is then able to translate (i.e. speckles appear to move in space while retaining their size and shape) or boil (i.e. no translation of the speckle but a continuous evolution from one size and shape to another). Speckle noise is produced if the Doppler signal amplitude remains high enough for the demodulator to operate. If the Doppler signal amplitude drops to low levels and the demodulation process fails, signal drop-out occurs. During its motion the valve is designed to rotate in order to keep the valve face and seat clean of carbon deposits. This also has the effect of slightly reducing the wear. Due to acting forces the valve also experiences tilt – especially at high speeds. All of these factors contribute to significant speckle noise during the valve kinematics measurement, as well as frequent drop-out noise.

We created a set of routines which were aimed at the recognition of signal drop-outs in the valve kinematics data. The developed algorithm helps to increase throughput of the engine test stand and decrease the time needed for evaluation of the valvetrains. The routines were tested on data which were collected for over 20 years and on data measured on combustion engines in our laboratory. The tests show satisfactory results in the identification of the phenomenon. Small drop-outs which are recognizable by the human eye might be on the edge of the algorithm's capabilities, especially if their size is not far from the estimated level of noise. The next step is to use the tests with different engines during everyday measurements in the ŠKODA AUTO laboratory, and to adjust the parameters if needed.

Thanks to the drop-out recognition tests, the measurement can be fully automated and repeated if necessary. The original measurement time of one valve has been shortened by 75%. Additional time saving is created by avoiding the manual repositioning of the IRC sensor if the IRC reference pulse would be generated during the opening/closing phase of the valve. The reference mark is supposed to trigger the measurements and reset the laser probes controller at every revolution. If it was generated during the opening/closing phase of the valve, it would start the acquisition at an unwanted position; and resetting the probes at this point would cause false reading. Our solution utilizes one programmable counter of the counter board for pulse generation. When the original trigger (reference pulse) arrives, it generates a new pulse with a predefined delay. The delay is specified as the amount of ticks of the source signal which is the IRC TTL pulse train. The operation is retriggerable.

To verify the proper function of the constructed apparatus and to adjust the parameters of the drop-out recognition tests, as well as to analyze and compare measured data of two different valvetrains, we measured the standard ŠKODA 1.2 HTP valvetrain and the low-friction version of the same valvetrain. Additional motivation was to verify the benefit of having the true camshaft speed fluctuations record for the valve acceleration computation. Common practice is to neglect the variance in rpm_{cam} and presume the rotational speed to be constant. The main reason is that the synchronized information about camshaft speed fluctuations is not usually available.

The achieved results were satisfactory proving the overall capabilities of the apparatus and the drop-out recognition tests. It is a great benefit to have the synchronized camshaft speed fluctuation information without utilizing another device. It is capable of revealing speeds critical for the valvetrain, (e.g. 5100 rpm for the ŠKODA 1.2 HTP valvetrain in a half-engine setup as a result of resonance of the timing chain). The performed analyses show two perfectly-working valvetrains with no malfunctions. The low-friction valvetrain achieves the same results with lower mass, different material of the cam lobes, thinner valve springs, smaller stiffness and different bearings. It operates with lower friction losses and thus requires less input power. An engine with such a valvetrain will have lower fuel consumption and will produce less emissions.

No valve float or valve bouncing was identified in either of both the measured data. The impact velocities, which is a crucial parameter for a valvetrain lifetime, were in the expected

range. The benefit of having the speed fluctuations data for the valve acceleration computation was not proved. There are insignificant differences between the acceleration obtained by presuming the speed of the shaft to be constant and by utilizing the speed fluctuations data. It is safe to say that in the case of modern valvetrains, rotational irregularities do not play a significant role in the valve acceleration calculation and the rotation can be simplified as a constant for this purpose.

The last part of our work was to carry out a comparison of the data measured by a *half-engine setup* and a *partial-engine setup,* which is preferred in industry. Instead of testing the complete engine, assembly of merely the head and head cover is used. Such a setup is easy to assemble and does not demand additional modifications of the components. At the same time the exchange of the valvetrain components is fast and the valves are easily optically accessible. On the other hand, it poses only a fraction of the original mass of the engine. Nevertheless, it was expected to deliver results close to the half-engine setup and thus close to the values of a real operating engine. Although the partial setup has become a widely used solution since the OHC valvetrains became standard, no direct comparison of the same valvetrain in half-engine and partial-engine setup has been published (to the author's knowledge). We conducted this comparison on a 3-cylinder ŠKODA 1.2 HTP engine first with a standard valvetrain and then with the low-friction version. The main focus was on the valve kinematic variables, but the two setups were also compared from the point of camshaft speed fluctuations.

It can be concluded that in most of the cases, the measured valve kinematics data of the partial-engine setup correlate with the data measured on the half-engine setup. However, there are some cases where legitimacy of the usage of the partial system could be questioned. At high speeds (5700-6000 rpm), the amplitude of the acceleration oscillations is significantly lower than what would be measured with the half-engine setup. It could lead to false conclusions about the necessary stiffness of the valve springs and valve behavior. These differences are most likely a direct result of the differences in the amplitude and phase of the speed fluctuations between the two setups.

The determined impact velocities do not significantly differ between the partial and the half-engine setup. From this point the partial-engine setup delivers correlated results.

As expected, the speed fluctuations of the two setups are very different. The higher camshaft speed fluctuations of the partial-engine setup are a result of lacking moving parts (and thus their inertia) and by driving only one camshaft at a time. To identify the exact origin of the differences in the speed fluctuations (amplitude, phase, orders) between the two setups we would need precise numerical models. To construct them is beyond the scope of this thesis and leaves door open for future research.

These measurements should be a significant source of information for the engineers in automotive industry and should contribute to the ongoing discussion about the modifications of the partial-engine setup. The updated version will most likely add a timing chain/timing belt in order to drive both the sprockets of the camshafts. The chain tensioner blade and a ‘dummy’ crankshaft sprocket will be positioned exactly as in a real-engine. Instead of driving the camshaft the crankshaft sprocket/pulley will be driven by the electromotor. The consequent measured valve kinematics should be closer to the values of a real engine.

7 List of original papers of the author

Papers in journals

I P. Hosek, T. Prykäri, E. Alarousu and R. Myllylä, Application of LabVIEW: Complex Software Controlling of System for Optical Coherence Tomography Using LabVIEW, Journal of the Association for Laboratory Automation, April 2009, Volume 14, Issue 2, pp. 59-68.
The software design patterns described in this paper were used to create the final application for valvetrain measurements developed as a part of this thesis.

II P. Hosek, M. Diblik: Implementation of Siemens USS Protocol into LabVIEW, Journal of the Association for Laboratory Automation, October 2011, Vol. 16, Issue 5, pp. 347-354

III P. Hosek, Algorithm for signal drop-out recognition in IC engine valve kinematics signal measured by laser Doppler vibrometer, Journal of Optics & Laser Technology, DOI: 10.1016/j.optlastec.2011.09.034, accepted 9/2011

Papers in preparation

I P. Hosek, Comparison of camshaft speed fluctuations and valvetrain kinematics of engine in half setup and partial setup *(chapter 11 of the thesis)*

8 Publications referenced in the report

[1] Marcello Montanari, Fabio Ronchi, Carlo Rossi, and Alberto Tonielli, "Control of a Camless Engine Electromechanical Actuator: Position Reconstruction and Dynamic Performance Analysis," *IEEE transactions on industrial electronics*, vol. Vol 51, no. 2, April 2004.

[2] Y. Wang, A. Stefanopoulou, K. Peterson, T. Megli, and M. Haghgooie, "Modeling and control of electromechanical valve actuator," *SAE Paper 2002–01–1106*, 2002.

[3] D. Kim, M. Anderson, T. Tsao, and M. Levin, "A dynamic model of a springless electrohydraulic camless valvetrain systems," *SAE Paper 970 248*, 1997.

[4] Fiat Group Automobiles S.p.A., "Adaptive control system of the air-fuel ratio of an internal combustione engine with a variable valve timing system," EP 2 204 566 A1, Dec. 29, 2008.

[5] T. D. Choi, O. J. Eslinger, C. T. Kelley, J. W. David, and M Etheridge, "Optimization of Automotive Valve Train Components with Implicit Filtering," *Optimization and Engineering*, vol. Volume 1, Number 1 / June, 2000, pp. 9-27, June 2000.

[6] Andrea Carlini, Allessandro Rivola, Giorgio Dalpiaz, and Alberto Maggiore, "Valve motion measurements on motorbike cylinder heads using high-speed laser vibrometer," in *Proc. SPIE Vol. 4827, Fifth International Conference on Vibration Measurements by Laser Techniques:* , Ancona, Italy, Tuesday 18 June 2002, pp. p. 564-574.

[7] Petr Hošek, Analysis of kinematic variables of valve train, diploma thesis (in Czech), 2006, TUL.

[8] M. Gasparetti, N. Paone, and E. P. Tomasini, "Laser Doppler techniques for the combined measurement of inlet flow and valve motion in IC engines," *Measurement Science and Technology*, no. Volume 7, Number 4, April 1996.

[9] B. F. Payne and Charles Federman, "An automated fringe counting laser interferometer for low frequency vibration measurements," *International Instrumentation Symposium*, pp. p. 1-7, 1986.

[10] H. Selbach, A.C. Lewin, and V. Roth, "Laser Doppler-vibrometer for applications in the automotive industry," in *Proceedings 25th ISATA Silver Jubilee International Symposium on Automotive Industry*, Florence, Italy, 1992.

[11] S.J. Rothberg and Halliwell, N.A. Baker, "Laser vibrometry: pseudo-vibrations," *Journal of Sound and Vibrations*, no. 135(3), pp. 516-522, 1989.

[12] Peter Martin and Steve Rothberg, "Introducing speckle noise maps for Laser Vibrometry," *Optics and Lasers in Engineering*, no. 47, pp. 431-442, 2009.

[13] Peter Martin and Steven, J. Rothberg, "Pseudo-vibration sensitivities for commercial laser vibrometers," *Mechanical Systems and Signal Processing*, vol. 25, no. 7, pp. 2753-2765, October 2011.

[14] Harold Rothbart, *Cam Design Handbook: Dynamics and Accuracy*, 1st ed.: McGraw-Hill Professional, October 23, 2003.

[15] A. P. Pisano and F. Freudenstein, "An Experimental and Analytical Investigation of the Dynamic Response of a High-Speed Cam-Follower System. Part 1: Experimental Investigation," *Journal of Mechanisms, Transmissions and Automation in Design*, no. 105, pp. pp.692–698, 1983.

[16] N. Takai, T. Iwai, and T. Asakura, "Correlation distance of dynamic speckles," *Applied*

Optics, vol. 22, no. 1, pp. 170-177, 1983.

[17] Takashi Nakamura and Toshimitsu Asakuraa, "Statistical properties of dynamic speckles produced by a curved surface," *Optics Communications*, vol. 98, no. 4-6, pp. 331-339, May 1993.

[18] Victor Hillier and Peter Coombes, *Fundamentals of motor vehicle technology*, 5th ed.: Nelson Thornes.

[19] G. Agostinelli, C. Cristalli, N. Paone, and S. Serafini, "Drop-out noise of laser vibrometers measuring on varnished steel surfaces of appliance cabinets for industrial diagnostics," in *9th International conference on vibration measurements by laser and non-contact techniques and short course*, May 28, 2010, pp. 298-312.

[20] J. Vass, R. Šmíd, R.B. Randall, P. Sovka, C Cristalli, and B Torcianti, "Avoidance of speckle noise in laser vibrometry by the use of kurtosis ratio: Application to mechanical fault diagnostics," *Mechanical Systems and Signal Processing*, vol. 22, pp. 647–671, 2008.

[21] Polytec, OFV-3001 Laser Vibrometer Controller (Datasheet).

[22] F. E. Grubbs, "Procedures for detecting outlying observations in samples," *Technometrics*, no. 11, pp. 1-21, 1969.

[23] Shu-Ho Dai and Ming-O Wang, *Reliability analysis in engineering applications*. New York: Van Nostrand Reinhold, 1992.

[24] J. H. McClellan and T. W. Parks, "A Personal History of the Parks–McClellan Algorithm," *Signal Processing Magazine, IEEE*, vol. 22, no. 2, March 2005.

[25] G. Taylor and T. Campbell, "Design analysis of cam and tapped interaction for wear reduction in marine diesel engines," *Society of Automotive Engineering (SAE)*, vol. vol. 3, p. 8, 1989.

[26] M. Roskilly and et al., "Valve Gear Design Analysis," *Society of Automotive Engineering*, vol. vol. 3, 1986.

[27] P. Kreuter and G. Mass, "Influence of Hydraulic Valve Lash Adjusters on the Dynamic Behavior of Valve Trains," *Society of Automotive Engineering*, 1987.

[28] M. Husselman, Modeling and verification of valve train dynamics in engines, 2005, Phd Thesis.